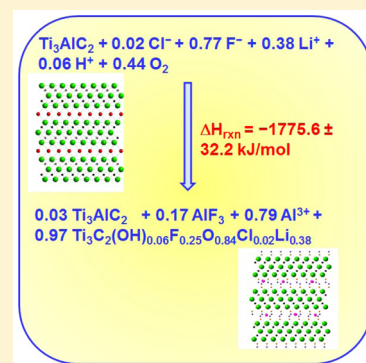


Calorimetric Determination of Thermodynamic Stability of MAX and MXene Phases

Geetu Sharma,[†] Michael Naguib,[‡] Dawei Feng,[†] Yury Gogotsi,[§] and Alexandra Navrotsky^{*,†,§}[†]Peter A. Rock Thermochemistry Laboratory, NEAT-ORU, University of California Davis, Davis, California 95616, United States[‡]Materials Science and Technology Division, Oak Ridge National Laboratory, Oak Ridge, Tennessee 37381, United States[§]Department of Materials Science and Engineering and A. J. Drexel Nanomaterials Institute, Drexel University, Philadelphia, Pennsylvania 19104, United States

Supporting Information

ABSTRACT: MXenes are layered two-dimensional materials with exciting properties useful to a wide range of energy applications. They are derived from ceramics (MAX phases) by leaching, and their properties reflect their resulting complex compositions which include intercalating cations and anions and water. Their thermodynamic stability is likely linked to these functional groups but has not yet been addressed by quantitative experimental measurements. We report enthalpies of formation from the elements at 25 °C measured using high temperature oxide melt solution calorimetry for a layered Ti–Al–C MAX phase, and the corresponding Ti–C based MXene. The thermodynamic stability of the $Ti_3C_2T_x$ MXene (T_x stands for anionic surface moieties, and intercalated cations) was assessed by calculating the enthalpy of reaction of the MAX phase (ideal composition Ti_3AlC_2) to form MXene. The very exothermic enthalpy of reaction confirms the stability of MXene in an aqueous environment. The surface terminations (O, OH, and F) and cations (Li) chemisorbed on the surface and intercalated in the interlayers play a major role in the thermodynamic stabilization of MXene. These findings help in understanding and potentially improving properties and performance by characterizing the energetics of species binding to MXene surfaces during synthesis and in energy storage, water desalination, and other applications.



INTRODUCTION

Recently, two-dimensional (2D) materials with high aspect ratios and only a few atomic layers in thickness have been explored extensively because of their unique electronic and other properties.¹ In addition to graphene, several new classes of 2D materials such as hexagonal boron nitride,² transition metal dichalcogenides,³ and metal oxides⁴ have been studied. Because of their high surface area and attractive properties, metallic and semiconducting 2D materials are considered for applications in electrochemical energy storage, hydrogen storage, and thermoelectrics.⁵ In 2011, a new family of stacked 2D materials called MXenes was reported. The first MXenes were produced from the parent ternary layered MAX phases ($M_{n+1}AX_n$, M = early transition metal, A = group IIIA or IVA element, and X = carbon and/or nitrogen) by selective etching of the A layers to form 2D blocks of transition metal carbides.⁶ Because they have lamellar structures and 2D morphology analogous to graphene, this new family of 2D materials was termed “MXenes”.⁶ An idealized composition can be written for example $Ti_3C_2T_x$, but in reality, as explained below, MXenes are complex materials of variable composition.

MXenes exhibit promising performance in many applications such as supercapacitors,⁷ Li-ion batteries,⁸ water purification,⁹ sensors,¹⁰ and electronic devices.¹¹ Theoretical studies also predicted that some members of the MXene family can be used in hydrogen storage¹² and thermoelectric applications.¹³

To understand and predict MXene behavior and to facilitate their manufacturing and use knowledge of their composition, chemical termination of their surfaces and their interlayer chemistry is essential. Such properties depend on their conditions of synthesis, further processing, and operation and in turn affect their performance. It has been suggested that atoms, molecules, or ions which are chemically adsorbed on the surface during synthesis play a vital role in their stability, overall stoichiometry, and properties.¹⁴ It has been shown that some polar organic molecules and ions can also intercalate in the lamellar structure, and subsequently affect the interlayer spacing, surface chemistry, and properties of MXenes.¹⁵ To date, about 20 MXenes have been reported, and the most widely studied among them has the approximate formula $Ti_3C_2T_x$, where T denotes surface termination, usually OH^- , O^{2-} , and/or F^- due to the aqueous HF treatment.^{6,16–19} The synthesis of MXenes from the corresponding MAX phases uses hydrofluoric acid, HF, or a mixture of fluoride salts and inorganic acids, such as HCl, as etchants.^{6,20} However, on using aqueous solutions of LiF and HCl, the resulting $Ti_3C_2T_x$ exhibits clay-like properties and swells in volume when hydrated.²⁰ NMR experiments reveal that, using LiF–HCl

Received: October 10, 2016

Revised: November 18, 2016

Published: November 19, 2016

etching, the resulting MXene shows a lower content of OH and F terminations and a higher content of O-terminations.²¹ Lithium ions can also intercalate between the layers. Hence, this method is highly preferred for producing MXenes for use in Li-ion and other batteries where O-terminations tend to give higher capacity.^{8,20} This method of MXene production provides a new versatile pathway for various studies.

The layers in the lamellar structure of MXenes are held together by a mixture of hydrogen and van der Waals forces,²² typically caused by polarizable, nonmetallic groups bound on their surfaces on exposure to the acidic solution.^{6,15} The multilayered structure of MXenes can be mechanically separated by ultrasonication to form single- or few-layer MXene flakes suspended in solution.⁶ After filtration, one can isolate freestanding single-layer MXene flakes.⁶ Given their prospects in various applications, it is surprising that, to date, there are few systematic characterizations of surface groups of MXenes.^{21–24}

MXenes have been predicted to have high thermodynamic stability.²⁵ However, no directly measured values of energetics by standard experimental techniques have been reported. Hence, it is highly desirable to investigate thermodynamic properties of a MXene sample with known composition.

In view of the unique and practically useful properties of MXenes synthesized using LiF–HCl as an etchant, in the present study, a particular clay-like MXene has been chosen in the present work to study the energetics of formation from the corresponding MAX phase by direct calorimetric measurements. We report the formation enthalpies of $Ti_3C_2T_x$ MXene (the exact chemical composition of the samples studied is $Ti_3Al_{0.21}C_2O_{0.81}(OH)_{0.06}F_{0.77}Cl_{0.02}Li_{0.38}$), and the parent Ti_3AlC_2 MAX phase (the exact composition of the sample is $Ti_3Al_{1.14}C_2O_{0.21}$), based on high temperature oxide melt solution calorimetry. We conclude that the formation of MXene from the parent MAX phase is highly energetically favorable in aqueous solution, and the chemical groups on the surface and intercalated ions play a major role in the thermodynamics of reaction.

■ EXPERIMENTAL METHODS

Synthesis. To synthesize Ti_3AlC_2 , TiC powder (2 μm particle size, 99.5%, Alfa Aesar) and Ti_2AlC (<38 μm , 95%, Kanthal) with a molar ratio of 1:1 were mixed in a high-density polyethylene (HDPE) jar with zirconia balls using a Turbula shaker–mixer for 4 h. Then, the mixture was transferred to an alumina crucible and heated to 1350 °C at 10 °C/min and held at that temperature for 2 h. Afterward, the sample was allowed to cool inside the furnace until it reached room temperature. The thermal cycle was carried out in a tube furnace under a continuous flow of high purity argon. The clay-like MXene was synthesized following the reported procedure.²⁰ Briefly, 3 g of Ti_3AlC_2 powder (<38 μm) was slowly added to a solution of 2 g of LiF (99.98%, Alfa Aesar) dissolved in 30 mL of 6 M aqueous HCl (37%, Sigma-Aldrich); the mixture was heated for 45 h at 40 °C with continuous stirring. After etching, the resulting sediments were washed several times with deionized (DI) water, centrifuged, and decanted to achieve a pH of the supernatant close to 6. Finally, the obtained product was dried at room temperature using a vacuum-assisted filtration device.

Elemental Analysis. The MAX and MXene samples were analyzed using inductively coupled plasma optical emission spectroscopy (ICP-OES), while carbon, oxygen, and sulfur

contents were determined using a combustion/IR technique. ICP-OES and the combustion/IR technique were conducted by Element Materials Technology, New Berlin, WI. The fluorine and chlorine contents were determined by SF Analytical Europhins Lab, New Berlin, WI, using method MIL-STD-2041. To evaluate the Li content of the MXene, a known quantity of MXene sample was digested in 20% HNO_3 and was completely oxidized, yielding a colorless powder (oxidation to TiO_2) after overnight stirring at room temperature. The system was then centrifuged to isolate the solid, and three dilutions in the 100–1000 ppb range were made of the supernatant and analyzed by the UC Davis/Interdisciplinary Center for Plasma Mass Spectrometry using an Agilent 7500CE inductively coupled plasma mass spectrometer (ICP-MS; Agilent Technologies, Palo Alto, CA). The samples were introduced using a MicroMist nebulizer (Glass Expansion, Pocasset, MA) into a temperature-controlled spray chamber with helium as the collision cell gas. Instrument standards were diluted from Certiprep ME 2A (SPEX CertiPrep, Metuchen, NJ) to 0.5, 1, 10, 100, 200, 500, 1000, 2000, and 5000 mg/L respectively in 3% trace element HNO_3 (Fisher Scientific) in 18.2 Mohm-cm water. A NIST 1643E Standard (National Institute of Standards and Technology, Gaithersburg, MD) was analyzed initially and QC standards consisting of an ME 2A at a concentration of 100 mg/L were analyzed every 12th sample as quality controls. The average Li value obtained from three dilutions from ICP-MS was used in the calculations.

High Temperature Oxide Melt Solution Calorimetry.

To determine the thermodynamic properties of MAX and MXene phases, high temperature solution calorimetry measurements were performed in an AlexSYS isoperibol Tian-Calvet twin microcalorimeter. The details of the microcalorimeter and experimental procedures have been described elsewhere in detail.^{26,27} In this method, the sample is oxidized to TiO_2 , which dissolves in the molten oxide calorimetric solvent, and the alkali metal halide impurities also dissolve, while carbon is evolved as CO_2 gas and H_2O and OH species are evolved as gaseous water. Typically, samples were loosely hand-pressed into pellets of about 1.5 mg, weighed, and dropped from room temperature into the molten solvent ($3Na_2O \cdot MoO_3$) in a platinum crucible in the calorimeter at 802 °C. Measurements were repeated eight times to achieve statistically reliable data. The calorimeter assembly was flushed with oxygen (40 mL/min) to drive off any evolved gases during dissolution. Oxygen was bubbled through the solvent at 5 mL/min to speed up oxidation, aid dissolution, and prevent local saturation. The calorimeter was calibrated using the heat content of ~ 5 mg of corundum pellets dropped into an empty Pt crucible as a standard protocol.

■ RESULTS AND DISCUSSION

Figure 1 shows a schematic representation of the crystal structures of MAX and MXene. For simplicity, the structures of MAX and MXene are represented as Ti_3AlC_2 and $Ti_3C_2(OH)_2$, respectively. In Ti_3AlC_2 , which is a layered hexagonal material, nearly close-packed Ti layers are interleaved with Al layers and the C atoms fill the octahedral sites between the former.⁶ On etching, the Al layers are replaced by various surface terminations and some species from the aqueous solution also intercalate between the layers of 2D MXene sheets.

Based on the chemical analyses, the MAX sample composition is $Ti_3Al_{1.14}C_2O_{0.21}$. The presence of oxygen and excess aluminum relative to the ideal composition Ti_3AlC_2

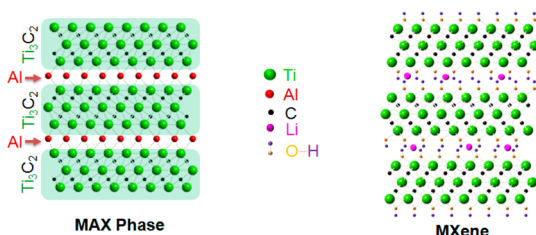


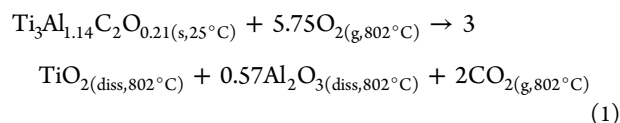
Figure 1. Schematic representation showing the crystal structures of MAX and MXene. For simplicity, MAX is shown as Ti_3AlC_2 and MXene is shown as $\text{Ti}_3\text{C}_2(\text{OH})_2$. Real systems are compositionally much more complex and the actual reaction measured here is $(\text{Ti}_3\text{Al}_{1.14}\text{C}_2\text{O}_{0.21} + 0.02\text{Cl}^- + 0.77\text{F}^- + 0.38\text{Li}^+ + 0.06\text{H}^+ + 0.66/2\text{O}_2 \rightarrow \text{Ti}_3\text{Al}_{0.21}\text{C}_2\text{O}_{0.81}(\text{OH})_{0.06}\text{F}_{0.77}\text{Cl}_{0.02}\text{Li}_{0.38} + 0.93\text{Al}^{3+})$, with further corrections, see below, made for phase impurities.

probably comes from the 6.47 mol % Al_2O_3 determined from X-ray diffraction (XRD) analysis. The analyzed total chemical composition of the MXene sample is $\text{Ti}_3\text{Al}_{0.21}\text{C}_2\text{O}_{0.81}(\text{OH})_{0.06}\text{F}_{0.77}\text{Cl}_{0.02}\text{Li}_{0.38}$. The Li content was obtained from the ICP-MS analysis, while the Cl content was determined from the elemental analysis. The Al content was also obtained from the elemental analysis. It was 17.47 mol % after HCl–LiF etching and dropped to 3.3 mol % after HCl washing. Since all the fluoride salts should be dissolved during HCl washing, it is reasonable to assume that the entire remaining Al after HCl washing is in the form of unreacted Ti_3AlC_2 . The HCl washing was done to determine how much aluminum fluoride was present, but calorimetry was done on the water washed sample for which complete analytical data are available. This translates into 3.3 mol % Ti_3AlC_2 . Considering that Ti_3AlC_2 is resistive to HCl, its amount should be the same before and after HCl washing. Assuming that all remaining Al is in the form of AlF_3 , then the latter concentration in the sample would be ~ 14.85 mol %. Then the mole percent of unreacted Ti_3AlC_2 in the MXene sample before HCl washing would be 2.72 mol %. Finally, the calculated sample composition is 2.72 mol % Ti_3AlC_2 + 14.85 mol % AlF_3 + 82.43 mol % $\text{Ti}_3\text{C}_2(\text{OH})_{0.06}\text{F}_{0.25}\text{O}_{0.84}\text{Cl}_{0.02}\text{Li}_{0.38}$. The ratio of OH:F:O was estimated based on a previous NMR study for a sample prepared using the same conditions.²¹ A lesson learned in dealing with these complex materials is the paramount importance of reliable chemical analysis.

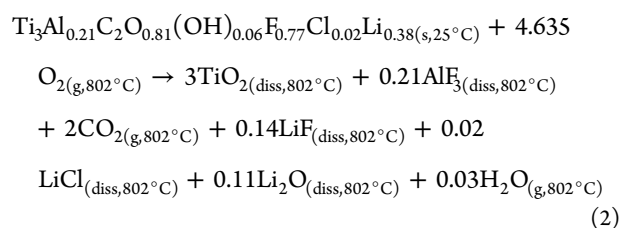
The drop solution enthalpies for MAX and MXene samples were obtained directly from high temperature oxide melt solution calorimetric experiments. Table 1 lists the enthalpies of drop solution at 802 °C along with calculated oxidation and formation enthalpies at 25 °C for MAX and MXene. These

calculations are shown for both the actual sample compositions and for the MAX and MXene compositions corrected for the assumed phase impurities. Both sets of values are given because the first refers to the actual data, while the second, though our best estimate for impurity content, may not be a unique representation. We also wish to evaluate the magnitude of the difference between these two calculations.

The calorimetric experiments measure the drop solution enthalpy (ΔH_{ds}) of the reaction shown in eqs 1 and 2 for the actual compositions of MAX and MXene samples.



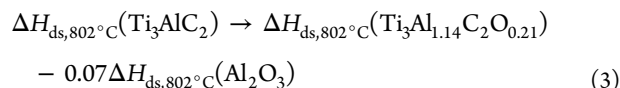
$$\Delta H_{\text{ds}, 802^\circ\text{C}} = -3834.10 \pm 31.51 \text{ kJ/mol}$$



$$\Delta H_{\text{ds}, 802^\circ\text{C}} = -1689.35 \pm 0.64 \text{ kJ/mol}$$

However, the MAX sample clearly contains an excess of aluminum and oxygen relative to the ideal Ti_3AlC_2 composition. Supported by the XRD data and the ratio of excess Al to O being close to 2/3, we believe that this represents a small amount of α -alumina as discussed above. We corrected for the Al_2O_3 impurity to obtain the enthalpy of drop solution and formation of stoichiometric Ti_3AlC_2 . Also, the effect of phase impurities for MXene has been corrected to obtain the enthalpy of drop solution, and oxidation and formation of $\text{Ti}_3\text{C}_2(\text{OH})_{0.06}\text{F}_{0.25}\text{O}_{0.84}\text{Cl}_{0.02}\text{Li}_{0.38}$, and are described below.

The drop solution enthalpy (ΔH_{ds}) corrected for phase impurities for the MAX and MXene phases are shown in eqs 3 and 4, respectively:

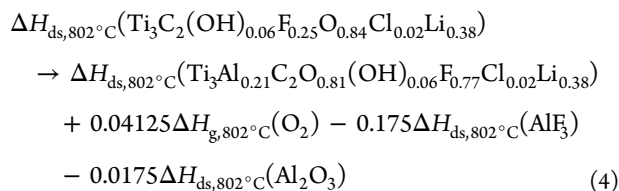


$$\Delta H_{\text{ds}, 802^\circ\text{C}}(\text{Ti}_3\text{AlC}_2) = -3841.85 \pm 31.51 \text{ kJ/mol}$$

Table 1. Measured and Calculated Oxidation Enthalpies and Formation Enthalpies for Parent MAX Phase and the Corresponding MXene^{a,b}

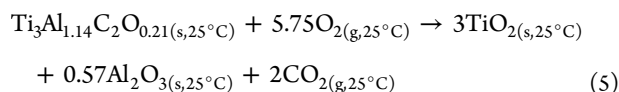
sample		$\Delta H_{\text{ds}, 802^\circ\text{C}}$ (kJ/mol)	$\Delta H_{\text{ox}, 25^\circ\text{C}}$ (kJ/mol)	$\Delta H_{\text{f}, 25^\circ\text{C}}$ (kJ/mol)
MAX	actual composition ($\text{Ti}_3\text{Al}_{1.14}\text{C}_2\text{O}_{0.21}$)	$-3834.10^d \pm 31.51$ (8) ^e	-4049.3 ± 31.7	-527.2 ± 32.0
	corrected composition (Ti_3AlC_2) ^f	-3841.85 ± 31.51	-4049.3 ± 31.7	-409.8 ± 31.9
MXene	actual composition ($\text{Ti}_3\text{Al}_{0.21}\text{C}_2\text{O}_{0.81}(\text{OH})_{0.06}\text{F}_{0.77}\text{Cl}_{0.02}\text{Li}_{0.38}$)	-1689.35 ± 0.64 (8) ^e	-1905.3 ± 3.7	-2202.1 ± 5.4
	corrected composition ($\text{Ti}_3\text{C}_2(\text{OH})_{0.06}\text{F}_{0.25}\text{O}_{0.84}\text{Cl}_{0.02}\text{Li}_{0.38}$) ^f	-1714.74 ± 0.67	-1917.0 ± 3.7	-1908.2 ± 5.4

^a ΔH_{ds} = enthalpy of drop solution; ΔH_{ox} = enthalpy of oxidation; ΔH_{f} = enthalpy of formation. The same abbreviations are used in all the tables in the Supporting Information. ^bErrors are expressed as two standard deviations of the average value. ^cValues calculated using enthalpy of formation of binary oxides from reference thermodynamic data. ^dAverage based on number of runs. ^eNumber in parentheses indicates number of measurements. ^fCorrected for phase impurities.

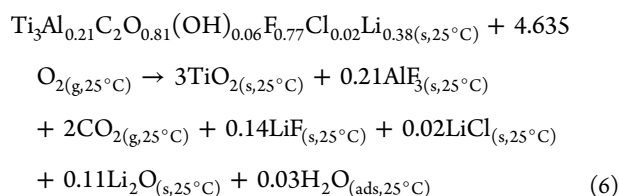


$$\Delta H_{\text{ds},802^\circ\text{C}} = -1714.74 \pm 0.67 \text{ kJ/mol}$$

The thermodynamic cycles in Tables S1 and S2 in the [Supporting Information](#) are used to calculate the enthalpies of oxidation at 25 °C. The oxidation enthalpies at room temperature refer to [reactions 5](#) and [6](#) for MAX phase and the corresponding MXene, respectively:

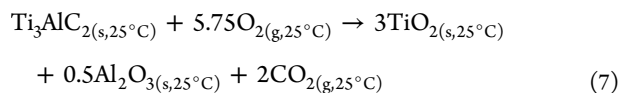


$$\Delta H_{\text{ox},25^\circ\text{C}} = -4049.3 \pm 31.7 \text{ kJ/mol}$$

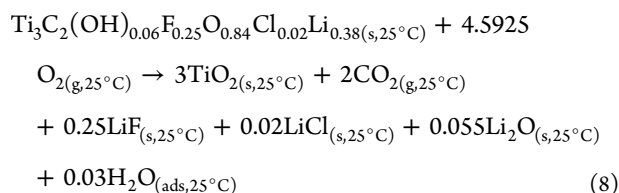


$$\Delta H_{\text{ox},25^\circ\text{C}} = -1905.3 \pm 3.7 \text{ kJ/mol}$$

The thermodynamic cycles in Tables S3 and S4 in the [Supporting Information](#) are used to calculate the enthalpies of oxidation at 25 °C for the corrected compositions of MAX and MXene as shown in [eqs 7](#) and [8](#), respectively:



$$\Delta H_{\text{ox},25^\circ\text{C}} = -4049.3 \pm 31.7 \text{ kJ/mol}$$

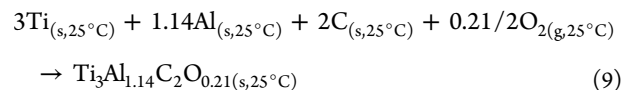


$$\Delta H_{\text{ox},25^\circ\text{C}} = -1917.0 \pm 3.7 \text{ kJ/mol}$$

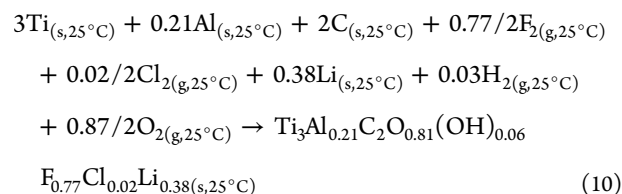
For both calculations (uncorrected and corrected for impurities), the MXene shows less exothermic enthalpy of drop solution and oxidation than its parent MAX. This is attributed to the stabilizing energetic effects of the functional groups, ions, or molecules present in the MXene after etching, as well as its significantly lower aluminum content. It has been reported that functional groups such as hydroxyl and carbonate present on the surface of metal oxides and nanodiamonds stabilize their surfaces, leading to less exothermic enthalpies of oxidation.²⁸ The MXene containing functional groups on its surface is already partially oxidized; therefore less heat is released on oxidation. This supports a theoretical investigation which suggests that all MXene surfaces prefer O binding more strongly than their parent MAX phases.²¹ Larger errors are

associated with enthalpy of drop solution of the MAX phase than with that of the MXene. These large errors are also associated with the enthalpy of formation of MAX, due to the propagation of errors.^{29,30} This larger error may reflect slower dissolution of the MAX than the MXene, consistent with the layered, nanophase, and partially oxidized nature of the latter. The scatter in data for the MAX may also reflect a heterogeneous distribution of the Al₂O₃ impurity phase. We note that preparing a 100% phase pure MAX is quite difficult, and we chose, in this initial study, to work with the best, though less than optimal, materials available to us.

Enthalpies of formation from elements were calculated for both MAX and MXene based on the thermochemical cycles in Tables S1 and S2 in the [Supporting Information](#), respectively. Thus, the formation enthalpy reactions for MAX and MXene can be written as shown in [eqs 9](#) and [10](#), respectively:

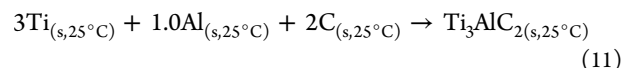


$$\Delta H_{\text{f},25^\circ\text{C}} = -527.2 \pm 32.0 \text{ kJ/mol}$$

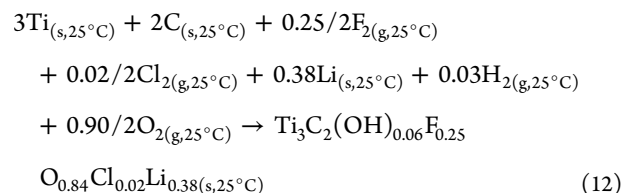


$$\Delta H_{\text{f},25^\circ\text{C}} = -2202.1 \pm 5.4 \text{ kJ/mol}$$

Enthalpies of formation from elements were also calculated for corrected compositions of MAX and MXene based on the thermochemical cycles in Tables S3 and S4 in the [Supporting Information](#) and are shown in [eqs 11](#) and [12](#):



$$\Delta H_{\text{f},25^\circ\text{C}} = -409.8 \pm 31.9 \text{ kJ/mol}$$



$$\Delta H_{\text{f},25^\circ\text{C}} = -1908.2 \pm 5.4 \text{ kJ/mol}$$

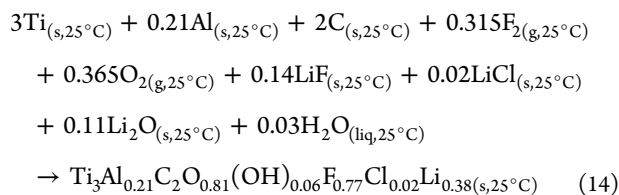
The impurity-corrected enthalpy of formation for the ideal MAX phase is close to that predicted for Ti₃AlC₂ by Dahlqvist et al.³¹ (−427 kJ/mol) using ab initio calculations. It is also comparable to the formation enthalpies of Ti₃AlC₂ estimated by Witusiewicz et al.³² (−418 kJ/mol), based on thermodynamic optimization of both experimental and calculated properties using the CALPHAD approach. Considering that Ti₃AlC₂ can be formed from TiAl + 2TiC, the enthalpies of formation of the binary carbides are important in understanding its stability. The enthalpy of formation of TiC is reported as ΔH_f = −180.9 kJ/mol, using first principles calculations based on density functional theory (DFT),³³ whereas the enthalpy of formation for TiAl was determined as −78.0 kJ/mol using

binary phase diagram parameters.³⁴ Therefore, the enthalpy of formation of a mechanical mixture of 2TiC + TiAl from the elements is -439.8 kJ/mol. In comparison, our results show the enthalpy of formation from elements for the ideal MAX phase (Ti_3AlC_2) to be -409.8 ± 31.9 kJ/mol which is within the margin of error. Since Ti_3AlC_2 can be synthesized using Ti_2AlC_2 and TiC, it is worthwhile to compare the measured ΔH_f for Ti_3AlC_2 and those of Ti_2AlC and TiC. Ti_2AlC is predicted to have $\Delta H_f = -258.4$ kJ/mol.³⁵ Therefore, the enthalpy of formation of a mechanical mixture of $\text{Ti}_2\text{AlC} + \text{TiC}$ would be -439.3 kJ/mol, which is very close to the measured value of Ti_3AlC_2 (-409.8 ± 31.9 kJ/mol). Thus, Ti_3AlC_2 appears to show a similar enthalpy of formation value as a mixture of Ti_2AlC and TiC; i.e., the reaction



does not have a strong energetic driving force. The observation that Ti_2AlC can be synthesized from this mixture confirms that the reaction must have a slightly negative free energy at the synthesis temperature.

The formation enthalpy of the MXene at 25 °C is calculated from elements Ti, Al, and C plus LiCl, LiF, and H_2O ; see Table S5. This formation reaction can be written as



$$\Delta H_{f,25^\circ\text{C}} = -2033.2 \pm 5.4 \text{ kJ/mol}$$

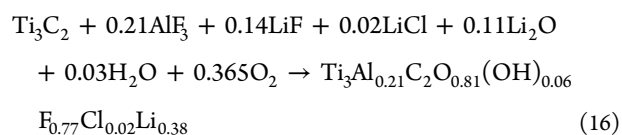
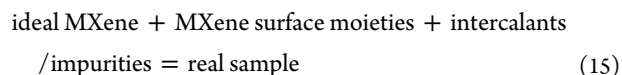
Reaction 14 eliminates from consideration the exothermic formation enthalpies of H_2O , LiCl, LiF, and Li_2O . Even with these exothermic contributions subtracted, the formation enthalpy of the MXene remains much more exothermic than that of the MAX, confirming the enhanced stability of the MXene compared to the MAX phase (both on the basis of 3 mol of Ti).

It would indeed be highly desirable to compare the theoretical DFT calculated enthalpy of formation of the ideal MXene (Ti_3C_2) with an experimental value for this ideal composition. However, all MXenes synthesized to date have the replacement of etched Al layers by hydroxyl, fluorine, or various other termination groups. Etching with LiF–HCl also causes some Li ions to intercalate in the MXene layers. Not knowing the strength of interaction of these various species with the MXene, we cannot correct uniquely for their energetic effects on the heat of formation. However, taking the DFT calculated enthalpy of formation of Ti_3C_2 as a starting point, we can estimate the overall enthalpy of interaction of the ideal (nonterminated) MXene and its terminating moieties, though we cannot identify the effect of each species separately. The reported enthalpy of formation of ideal unterminated Ti_3C_2 from the elements, based on DFT calculations, is -0.365 eV/atom,¹⁹ which is equal to -176.15 kJ/mol (five atoms in the Ti_3C_2 formula unit).

Ashton et al.²⁵ calculated from first principles the enthalpies of formation and surface compositions and binding energies of surface species for simplified MXene compositions having different metal atoms and layer thicknesses. They concluded that under typical synthesis conditions the MXene layers should

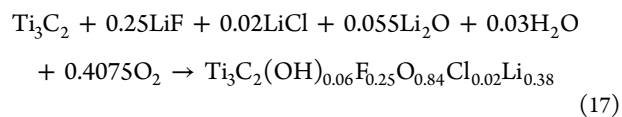
be preferentially saturated with oxygen. They also calculated enthalpies of formation which, when referenced to the elements, are -1233 , -1843 , and -1191 kJ/mol for $\text{Ti}_3\text{C}_2\text{O}_2$, $\text{Ti}_3\text{C}_2\text{F}_2$, and $\text{Ti}_3\text{C}_2(\text{OH})_2$, respectively, where the O_2 , F_2 , and $(\text{OH})_2$ refer to the terminating groups. For our sample, with corrected composition $\text{Ti}_3\text{C}_2(\text{OH})_{0.06}\text{F}_{0.25}\text{O}_{0.84}\text{Cl}_{0.02}\text{Li}_{0.38}$, $\Delta H_{f,\text{el}} = -1908$ kJ/mol. This somewhat more exothermic value probably reflects differences in composition, including the presence of lithium ions.

Then for the reaction



$$\begin{aligned} \Delta H_{\text{reaction},25^\circ\text{C}} &= \Delta H_f(\text{Ti}_3\text{Al}_{0.21}\text{C}_2\text{O}_{0.81}(\text{OH})_{0.06} \\ & \text{F}_{0.77}\text{Cl}_{0.02}\text{Li}_{0.38}) - [\Delta H_{f,25^\circ\text{C}}(\text{Ti}_3\text{C}_2) + 0.21\Delta H_f(\text{AlF}_3) \\ & + 0.14\Delta H_f(\text{LiF}) + 0.02\Delta H_f(\text{LiCl}) + 0.11\Delta H_f(\text{Li}_2\text{O}) \\ & + 0.03\Delta H_f(\text{H}_2\text{O}) + 0.365\Delta H_f(\text{O}_2)] \\ & = -1539.8 \text{ kJ/mol} \end{aligned}$$

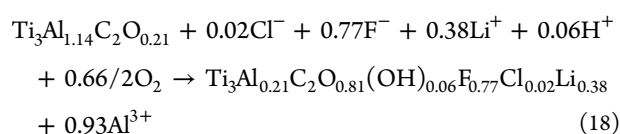
Similar to the above, the enthalpy of reaction is calculated for the corrected MXene and is shown in eq 17:



$$\begin{aligned} \Delta H_{\text{reaction},25^\circ\text{C}} &= \Delta H_f(\text{Ti}_3\text{C}_2(\text{OH})_{0.06}\text{F}_{0.25}\text{O}_{0.84}\text{Cl}_{0.02}\text{Li}_{0.38}) \\ & - [\Delta H_{f,25^\circ\text{C}}(\text{Ti}_3\text{C}_2) + 0.25\Delta H_f(\text{LiF}) + 0.02\Delta H_f(\text{LiCl}) \\ & + 0.055\Delta H_f(\text{Li}_2\text{O}) + 0.03\Delta H_f(\text{H}_2\text{O}) \\ & + 0.4075\Delta H_f(\text{O}_2)] = -1528.2 \text{ kJ/mol} \end{aligned}$$

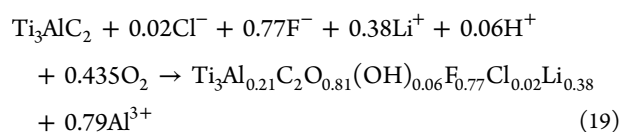
This calculation confirms the strongly stabilizing influence of the anionic and cationic substituents. Furthermore, it shows that the correction for impurities does not change the enthalpy significantly. In addition, even if the enthalpy of formation of Ti_3C_2 MXene calculated by DFT might have an uncertainty of 10–20%, this conclusion of a strongly exothermic reaction is robust. Thus, the MXene is strongly stabilized by its surface groups, which must be considered important constituents and not simply accidental impurities. This observation supports the absence of nonfunctionalized MXene phases after wet chemical synthesis. Further thermochemical studies of fully chemically characterized MXenes with different preparation histories and surface terminations would provide insight into the individual interactions of different species.

Using the enthalpy of formation values for the MAX and MXene listed in Tables S1 and S2 in the Supporting Information, and reference thermodynamic data, we also calculated the net enthalpy of reaction 18 (see Table S6 in the Supporting Information for the thermodynamic values used):



$$\Delta H_{\text{rxn},\text{sol},25^\circ\text{C}} = -1808.3 \pm 32.5 \text{ kJ/mol}$$

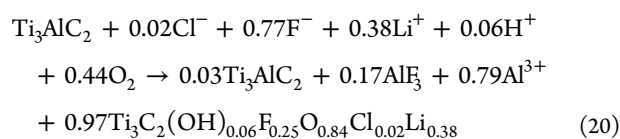
Similarly, the net enthalpy of reaction is also calculated using the enthalpy of formation value for the stoichiometric MAX phase; see Table S7 in the [Supporting Information](#). This enthalpy of reaction can be written as



$$\Delta H_{\text{rxn},\text{sol},25^\circ\text{C}} = -1850.3 \pm 32.4 \text{ kJ/mol}$$

This reaction is also strongly exothermic. The correction for impurities in the MAX phase does not change the value much.

The enthalpy of reaction in aqueous medium is also calculated using the enthalpy of formation value for the stoichiometric MAX phase and corrected MXene; see Table S8 in the [Supporting Information](#).



$$\Delta H_{\text{rxn},\text{sol},25^\circ\text{C}} = -1775.6 \pm 32.2 \text{ kJ/mol}$$

Again this value is similar to the others calculated above. We conclude that reasonably robust data can be obtained despite the possible uncertainties introduced by the impurities.

The reaction of the MAX phase to form MXene during aqueous etching involves breaking of metal–metal and metal–carbon bonds. Because Ti–Al bonds are weaker than Ti–C bonds, there is a selective loss of Al layers while etching (see [Figure 1](#)). In this process, Al atoms are replaced by O, OH, or F ions.³⁶ Additionally, the removal of Al layers dramatically weakens the interactions between the titanium carbide layers (i.e., MXene layers), allowing Li⁺ and other species from the aqueous solution to intercalate between the layers. However, in this MXene sample, there is still some Al present after etching. The source of this aluminum is attributed to the unreacted MAX phase or some unwashed aluminum fluoride salt formed during the etching process. Nevertheless, the formation of this MXene is highly exothermic and again confirms that the terminating groups and intercalated ions contribute strongly to the greater stability of the MXene than the MAX phase.

This work emphasizes the importance of termination and intercalated ions in the stabilization of MXene. Other etching conditions may produce MXene samples of different total compositions and having different thermodynamic properties, even though we expect the general trends to be the same. To understand the energetics of such processes, one must carefully and completely characterize the composition and structure of the MXene samples formed. We stress it is critical to include the surface adsorbed and interlayer (intercalated) cations (Li) and anions (F, Cl, OH) in the calculation of thermodynamic properties as they contribute significantly to the stability and

properties of the MXene. Thus, accurate chemical analysis is essential in any future thermochemical studies.

CONCLUSIONS

We have examined the energetics of Ti₃AlC₂ MAX phase and its corresponding MXene employing oxide melt solution calorimetry and complete chemical analysis. Enthalpy of formation of MXene from its parent MAX phase is highly exothermic, suggesting that LiF–HCl etching in aqueous solution produces a very stable MXene. The thermodynamic stability of MXene in contact with aqueous solution shows the importance of surface groups and lithium intercalation in the interlayers. Additional thermodynamic data on different MXenes are required to better understand their energetics in a complex compositional space as a function of transition metal, carbon-to-nitrogen ratio, and surface termination. This work provides a starting point for understanding MXene formation and evolution, which is critical for predicting its properties and performance in various applications.

ASSOCIATED CONTENT

Supporting Information

The Supporting Information is available free of charge on the ACS Publications website at DOI: [10.1021/acs.jpcc.6b10241](https://doi.org/10.1021/acs.jpcc.6b10241).

Thermodynamic tables for MAX and MXene phases (Tables S1–S8) ([PDF](#))

AUTHOR INFORMATION

Corresponding Author

*E-mail: anavrotsky@ucdavis.edu. Tel.: (530) 752-3292. Fax: (530) 752-9307.

ORCID

Alexandra Navrotsky: [0000-0002-3260-0364](https://orcid.org/0000-0002-3260-0364)

Notes

The authors declare no competing financial interest.

ACKNOWLEDGMENTS

This work was supported by the Fluid Interface Reactions, Structures & Transport, an Energy Frontier Research Center funded by the U.S. Department of Energy, Office of Science, Office of Basic Energy Sciences, under Award 4000134953.

REFERENCES

- (1) Shi, J.; Ji, Q.; Liu, Z.; Zhang, Y. Recent advances in controlling syntheses and energy related applications of MX₂ and MX₂/graphene heterostructures. *Adv. Energy Mater.* **2016**, *6*, 1600459.
- (2) Zhang, H. Ultrathin two-dimensional nanomaterials. *ACS Nano* **2015**, *9*, 9451–9469.
- (3) Coleman, J. N.; Lotya, M.; O'Neill, A.; Bergin, S. D.; King, P. J.; Khan, U.; Young, K.; Gaucher, A.; De, S.; Smith, R. J.; et al. Two-dimensional nanosheets produced by liquid exfoliation of layered materials. *Science* **2011**, *331*, 568–571.
- (4) Ma, R.; Sasaki, T. Nanosheets of oxides and hydroxides: Ultimate 2D charge-bearing functional crystallites. *Adv. Mater.* **2010**, *22*, 5082–5104.
- (5) Ahmed, B.; Anjum, D. H.; Hedhili, M. N.; Gogotsi, Y.; Alshareef, H. N. H₂O₂ assisted room temperature oxidation of Ti₂C MXene for Li-ion battery anodes. *Nanoscale* **2016**, *8*, 7580–7587.
- (6) Naguib, M.; Kurtoglu, M.; Presser, V.; Lu, J.; Niu, J.; Heon, M.; Hultman, L.; Gogotsi, Y.; Barsoum, M. W. Two-dimensional nanocrystals produced by exfoliation of Ti₃AlC₂. *Adv. Mater.* **2011**, *23*, 4248–4253.

- (7) Zhao, M. Q.; Ren, C. E.; Ling, Z.; Lukatskaya, M. R.; Zhang, C.; Van Aken, K. L.; Barsoum, M. W.; Gogotsi, Y. Flexible MXene/carbon nanotube composite paper with high volumetric capacitance. *Adv. Mater.* **2015**, *27*, 339–345.
- (8) Xie, Y.; Naguib, M.; Mochalin, V. N.; Barsoum, M. W.; Gogotsi, Y.; Yu, X.; Nam, K.-W.; Yang, X.-Q.; Kolesnikov, A. I.; Kent, P. R. Role of surface structure on Li-ion energy storage capacity of two-dimensional transition-metal carbides. *J. Am. Chem. Soc.* **2014**, *136*, 6385–6394.
- (9) Ying, Y.; Liu, Y.; Wang, X.; Mao, Y.; Cao, W.; Hu, P.; Peng, X. Two-dimensional titanium carbide for efficiently reductive removal of highly toxic chromium (VI) from water. *ACS Appl. Mater. Interfaces* **2015**, *7*, 1795–1803.
- (10) Zhang, J.; Wang, W.; Li, Y.; Yu, D. Y. W. Sodium storage capability of spinel $\text{Li}_4\text{Mn}_3\text{O}_{12}$. *Electrochim. Acta* **2015**, *185*, 76–82.
- (11) Lee, Y.; Hwang, Y.; Chung, Y.-C. Achieving type I, II, and III heterojunctions using functionalized MXene. *ACS Appl. Mater. Interfaces* **2015**, *7*, 7163–7169.
- (12) Hu, Q.; Sun, D.; Wu, Q.; Wang, H.; Wang, L.; Liu, B.; Zhou, A.; He, J. MXene: A new family of promising hydrogen storage medium. *J. Phys. Chem. A* **2013**, *117*, 14253–14260.
- (13) Khazaei, M.; Arai, M.; Sasaki, T.; Estili, M.; Sakka, Y. Two-dimensional molybdenum carbides: Potential thermoelectric materials of the MXene family. *Phys. Chem. Chem. Phys.* **2014**, *16*, 7841–7849.
- (14) Naguib, M.; Gogotsi, Y. Synthesis of two-dimensional materials by selective extraction. *Acc. Chem. Res.* **2015**, *48*, 128–135.
- (15) Mashtalir, O.; Naguib, M.; Mochalin, V. N.; Dall'Agnese, Y.; Heon, M.; Barsoum, M. W.; Gogotsi, Y. Intercalation and delamination of layered carbides and carbonitrides. *Nat. Commun.* **2013**, *4*, 1716.
- (16) Naguib, M.; Mashtalir, O.; Carle, J.; Presser, V.; Lu, J.; Hultman, L.; Gogotsi, Y.; Barsoum, M. W. Two-dimensional transition metal carbides. *ACS Nano* **2012**, *6*, 1322–1331.
- (17) Naguib, M.; Halim, J.; Lu, J.; Cook, K. M.; Hultman, L.; Gogotsi, Y.; Barsoum, M. W. New two-dimensional niobium and vanadium carbides as promising materials for Li-ion batteries. *J. Am. Chem. Soc.* **2013**, *135*, 15966–15969.
- (18) Ghidui, M.; Naguib, M.; Shi, C.; Mashtalir, O.; Pan, L.; Zhang, B.; Yang, J.; Gogotsi, Y.; Billinge, S. J.; Barsoum, M. W. Synthesis and characterization of two-dimensional Nb_4C_3 (MXene). *Chem. Commun.* **2014**, *50*, 9517–9520.
- (19) Anasori, B.; Xie, Y.; Beidaghi, M.; Lu, J.; Hosler, B. C.; Hultman, L.; Kent, P. R.; Gogotsi, Y.; Barsoum, M. W. Two-dimensional, ordered, double transition metals carbides (MXenes). *ACS Nano* **2015**, *9*, 9507–9516.
- (20) Ghidui, M.; Lukatskaya, M. R.; Zhao, M.-Q.; Gogotsi, Y.; Barsoum, M. W. Conductive two-dimensional titanium carbide/clay/ with high volumetric capacitance. *Nature* **2014**, *516*, 78–81.
- (21) Hope, M. A.; Forse, A. C.; Griffith, K. J.; Lukatskaya, M. R.; Ghidui, M.; Gogotsi, Y.; Grey, C. P. NMR reveals the surface functionalisation of Ti_3C_2 MXene. *Phys. Chem. Chem. Phys.* **2016**, *18*, 5099–5102.
- (22) Wang, H.-W.; Naguib, M.; Page, K.; Wesolowski, D. J.; Gogotsi, Y. Resolving the structure of $\text{Ti}_3\text{C}_2\text{T}_x$ MXenes through multilevel structural modeling of the atomic pair distribution function. *Chem. Mater.* **2016**, *28*, 349–359.
- (23) Halim, J.; Cook, K. M.; Naguib, M.; Eklund, P.; Gogotsi, Y.; Rosen, J.; Barsoum, M. W. X-ray photoelectron spectroscopy of select multi-layered transition metal carbides (MXenes). *Appl. Surf. Sci.* **2016**, *362*, 406–417.
- (24) Mashtalir, O.; Lukatskaya, M.; Kolesnikov, A.; Raymundo-Piñero, E.; Naguib, M.; Barsoum, M.; Gogotsi, Y. The effect of hydrazine intercalation on the structure and capacitance of 2D titanium carbide (MXene). *Nanoscale* **2016**, *8*, 9128–9133.
- (25) Ashton, M.; Mathew, K.; Hennig, R. G.; Sinnott, S. B. Predicted surface composition and thermodynamic stability of MXenes in solution. *J. Phys. Chem. C* **2016**, *120*, 3550–3556.
- (26) Navrotsky, A. Progress and new directions in high temperature calorimetry. *Phys. Chem. Miner.* **1977**, *2*, 89–104.
- (27) Navrotsky, A. Progress and new directions in high temperature calorimetry revisited. *Phys. Chem. Miner.* **1997**, *24*, 222–241.
- (28) Costa, G. C.; Shenderova, O.; Mochalin, V.; Gogotsi, Y.; Navrotsky, A. Thermochemistry of nanodiamond terminated by oxygen containing functional groups. *Carbon* **2014**, *80*, 544–550.
- (29) Cohen, E. An introduction to error analysis: the study of uncertainties in physical measurements. *Meas. Sci. Technol.* **1998**, *9*, 1015.
- (30) Allada, R. K.; Pless, J. D.; Nenoff, T. M.; Navrotsky, A. Thermochemistry of hydrotalcite-like phases intercalated with CO_3^{2-} , NO_3^- , Cl^- , I^- , and ReO_4^- . *Chem. Mater.* **2005**, *17*, 2455–2459.
- (31) Dahlqvist, M.; Alling, B.; Rosén, J. Stability trends of MAX phases from first principles. *Phys. Rev. B: Condens. Matter Mater. Phys.* **2010**, *81*, 220102.
- (32) Witusiewicz, V.; Hallstedt, B.; Bondar, A.; Hecht, U.; Sleptsov, S.; Velikanova, T. Y. Thermodynamic description of the Al–C–Ti system. *J. Alloys Compd.* **2015**, *623*, 480–496.
- (33) Liu, Y.; Jiang, Y.; Zhou, R.; Feng, J. First principles study the stability and mechanical properties of MC (M= Ti, V, Zr, Nb, Hf and Ta) compounds. *J. Alloys Compd.* **2014**, *582*, 500–504.
- (34) Hsieh, K.-C.; Chang, Y. A. Thermodynamic and structural parameters of the body-center tetragonal TiAl phase. *Scr. Metall.* **1988**, *22*, 1267–1272.
- (35) Duong, T.; Gibbons, S.; Kinra, R.; Arróyave, R. Ab-initio approach to the electronic, structural, elastic, and finite-temperature thermodynamic properties of Ti_2AX (A= Al or Ga and X= C or N). *J. Appl. Phys.* **2011**, *110*, 093504.
- (36) Naguib, M.; Mochalin, V. N.; Barsoum, M. W.; Gogotsi, Y. 25th Anniversary article: MXenes: A new family of two-dimensional materials. *Adv. Mater.* **2014**, *26*, 992–1005.